NEXT-TO-LEADING RESUMMED COEFFICIENT FUNCTION
FOR THE SHAPE FUNCTION

U. Aglietti[*]

Theoretical Physics Division, CERN
CH - 1211 Geneva 23

Abstract

We present a next-to-leading evaluation of the resummed coefficient function for the shape function. The results confirm our previous leading-order analysis, namely that the coefficient function is short-distance-dominated, and allow relating the shape function computed with a non-perturbative technique to the physical QCD distributions.

[*] On leave of absence from Dipartimento di Fisica, Universita' di Roma I, Piazzale Aldo Moro 2, 00185 Roma, Italy. E-mail address: ugo.aglietti@cern.ch.

1 Introduction

In this note we present a next-to-leading evaluation of the coefficient function of the shape function. The leading-order analysis was done in [1]. The coefficient function allows relating the shape function — computed with a non-perturbative technique — to physical distributions in semi-inclusive heavy-flavour decays.

In general, we consider the process

$$H_h \to X + (\mathrm{non-QCD\ partons}) \tag{1}$$

in the hard limit

$$Q \gg \Lambda \tag{2}$$

and in the semi-inclusive region[1]

$$M \ll Q, \tag{3}$$

where M is the invariant mass of X, the hadronic final state; H_h is a hadron containing a heavy quark h and the non-QCD partons can be a lepton pair, a vector boson, a photon, etc. The quantity Q is the hard scale of the time-like process: $Q \equiv 2\mathcal{E}$, where $\mathcal{E}$ is the final hadronic energy and Λ is the QCD scale. Well-known examples of (1) are:

$$B \to X_s + \gamma \tag{4}$$

for a large photon energy and

$$B \to X_u + l + \nu \tag{5}$$

for a small hadronic mass or a large electron energy[2].

For the hadron at rest, i.e. with velocity $v = (1; 0, 0, 0)$, and the jet X flying along the minus direction ($-z$ axis), the shape function is defined as [2]–[5]:

$$\varphi(k_+) \equiv \langle H_h(v) | h_v^\dagger \, \delta(k_+ - iD_+) \, h_v | H_h(v) \rangle. \tag{6}$$

The latter is also called structure function of the heavy flavour and represents the probability that the heavy quark in the hadron has momenta

$$p_h = m_H v + k \tag{7}$$

with any transverse and minus component and with given plus component k_+. The static field $h_v(x)$ is related to the Dirac field of the heavy quark $h(x)$ by:

$$h(x) = e^{-im_H v \cdot x} h_v(x) + O(\Lambda m_H). \tag{8}$$

---

[1]This region is also called threshold region, large-x region, radiation-inhibited region and Sudakov region.

[2]For the rare decay (4), since $Q = m_B \left(1 + m_{X_s}^2 / m_B^2\right)$, one can actually set $Q = m_B$.

With the shape function, the decay (1) is related to its respective quark-level process

$$h \to \widehat{X} + (\text{non} - \text{QCD partons}),\qquad (9)$$

where the heavy quark has the momentum (7) with the distribution (6). Note that the state $\widehat{X}$, unlike X, does not contain the light valence quark(s) in H. The invariant mass m of $\widehat{X}$ is related to the plus virtuality of the heavy quark k_+ by the relation:

$$k_+ = -m^2 Q.\qquad (10)$$

The shape function is a non-perturbative distribution — analogous to parton distribution functions — and it describes the slice of the semi-inclusive region in which

$$m^2 \sim \Lambda\, Q.$$

In terms of the variables used in QCD and in the effective theory (ET), this is:

$$k_+ \sim \Lambda, \qquad z \sim 1 - \Lambda Q, \qquad N \sim Q\Lambda,\qquad (11)$$

where

$$z \equiv 1 - m^2 Q^2,\qquad (12)$$

and N is the moment index (see later).

The shape function describes the mass distribution of a jet coming from the decay of a heavy flavour. It therefore generalizes to region (11) the jet function $J\left(Q^2, m^2\right)$ introduced in ref. [6], representing the probability that a light parton produced in a hard collision with scale Q evolves inclusively into a jet with mass m. The main difference is that in our case the distribution depends on the process as a whole, and not only on the fragmentation of the final quark. The shape function depends on the initial hadron state; for example, it is different for a B meson and a Λ_b hyperon.

The coefficient function C is defined by the relation[3]

$$\varphi\left(k_+; Q\right) = \int dk'_+\, C\left(k_+ - k'_+; Q, \mu\right)\, \varphi\left(k'_+; \mu\right),\qquad (13)$$

where μ is the renormalization point or UV cut-off of the operator entering the definition of the shape function (see eq. (6)). The coefficient function is then obtained by evaluating in next-to-leading order (NLO) the QCD effective form factor $\varphi\left(k_+; Q\right)$ and the shape function $\varphi\left(k_+; \mu\right)$ and taking their ratio (see later). Since C is expected to be a short-distance quantity, we compute the QCD distribution and the shape function in perturbation theory (PT) for an on-shell heavy quark $(k = 0)$. This expectation will be verified *a posteriori*.

The coefficient function is different, even at the leading level, for the shape function regulated in dimensional regularization (DR) and in lattice regularization; it is short-distance-dominated in both cases [7]. The main difference is that, at one loop, C contains a double logarithm of k_+ in DR, while it contains at most a single logarithm of k_+ in lattice regularization. In view of the applications, we specialize ourselves in the lattice case.

The paper is organized as follows. In sec. 2 we present a compact derivation of a resummed QCD form factor $\varphi\left(k_+; Q\right)$ to NLO accuracy. In sec. 3 we perform a similar computation for the shape function $\varphi\left(k_+; \mu\right)$. In sec. 4 we evaluate the coefficient function and we discuss the physical implications. Finally, in sec. 5, we draw our conclusions.

---

[3]QCD quantities are denoted by bold-face symbols, the related quantities in the ET by normal symbols.

2 The QCD distribution

We are interested in a general QCD distribution $\mathbf{f}(z)$ in the threshold region. For clarity's sake, let us consider a specific case: the photon spectrum in the decay (4),

$$\mathbf{f}(x) = 1\Gamma_B d\Gamma dx, \tag{14}$$

where

$$x \equiv 2E_\gamma m_b \tag{15}$$

and Γ_B is the Born width:

$$\Gamma_B = \alpha\pi G_F^2 m_b^5 32\pi^3 |V_{tb}V_{ts}^*|^2 |C_7(\mu_b)|^2. \tag{16}$$

The distribution reads, to order α_S [8]:

$$\mathbf{f}(x) = \overline{\mathbf{f}}(x) + \alpha_S\, k\, \delta(1-x) + \alpha_S\, d(x). \tag{17}$$

The function $\overline{\mathbf{f}}(x)$ factorizes (perturbative) long-distance effects occurring in (4) and reads:[4]

$$\overline{\mathbf{f}}(x) = \delta(1-x) - A_1\alpha_S \left(\log[1-x]\,1-x\right)_+ + B_1\alpha_S\,(11-x)_+\,, \tag{18}$$

where

$$A_1 = C_F\pi, \qquad B_1 = -74 C_F\pi \tag{19}$$

and $C_F = (N_c^2 - 1)/(2N_c) = 4/3$. The spike term involves the constant

$$k = -C_F\pi \left(\log \mu_b m_b + 54 + \pi^2 3\right), \tag{20}$$

where μ_b is the renormalization scale of the operator $\mathcal{O}_7$; this (unphysical) scale must be taken of $O(m_b)$ in order to avoid large (ultraviolet) logarithms in the matrix elements. The function $d(x)$ is the "remainder":

$$d(x) = C_F 4\pi \left[7 + x - 2x^2 - 2(1+x)\log(1-x)\right]. \tag{21}$$

Plus-distributions are defined as usual as $P(x)_+ \equiv P(x) - \delta(1-x)\int_0^1 dy\, P(y)$. For the resummation, it is natural to write the function $\overline{\mathbf{f}}(x)$ in an "unintegrated" form as

$$\overline{\mathbf{f}}(x) = \delta(1-x) + \int_0^1 d\epsilon \int_0^1 dt\,[A_1\alpha_S\epsilon t + S_1\alpha_S\epsilon + C_1\alpha_S t]\,[\delta(1-x-\epsilon t) - \delta(1-x)], \tag{22}$$

---

[4]Overlined quantities denote subtracted quantities, containing only infrared logarithms.

where we have defined the unitary energy and angular variables

$$\epsilon \equiv EQ \qquad \text{and} \qquad t \equiv 1 - \cos\theta 2. \tag{23}$$

The quantity E is two times the energy of the soft gluon, $E = 2E_g$, and θ is the gluon emission angle. It proves to be convenient to separate the soft from the collinear term, as we have done. By explicit evaluation, we find

$$S_1 = -C_F\pi, \qquad C_1 = -34C_F\pi. \tag{24}$$

Note that $B_1 = S_1 + C_1$, i.e. it is the sum of the coefficients of the soft and the collinear terms. Expression (22) is symmetric for $\varepsilon \leftrightarrow t$.

Next-to-leading corrections are included following these prescriptions:

1. Replacement of the bare coupling by the two-loop running coupling:

$$\alpha_s\left(q^2\right) = 1\beta_0 \log q^2/\Lambda^2 - \beta_1\beta_0^3 \log\log q^2/\Lambda^2 \log^2 q^2/\Lambda^2, \tag{25}$$

evalutated at the gluon transverse momentum squared [9]:

$$\alpha_S \to \alpha_S\left(k_\perp^2\right), \tag{26}$$

where

$$k_\perp^2 \simeq Q^2\epsilon^2 t. \tag{27}$$

The first two coefficients of the β-function are:

$$\begin{aligned}
\beta_0 &= 11C_A - 2n_F 12\pi = 33 - 2n_F 12\pi, \\
\beta_1 &= 17C_A^2 - 5C_A n_F - 3C_F n_F 24\pi^2 = 153 - 19\,n_F 24\pi^2,
\end{aligned} \tag{28}$$

where $C_A = N_c = 3$ and $n_F = 3$ is the number of active quark flavours;

2. Inclusion of the two-loop correction to the term $A_1\alpha_S$, so that

$$A_1\alpha_S \to A_1\alpha_S + A_2\alpha_S^2. \tag{29}$$

The explicit computation gives [10, 6]

$$A_2 = 12C_F\pi^2 K \tag{30}$$

where, in the $\overline{MS}$ scheme for the coupling constant,

$$K = C_A\left(6718 - \pi^2 6\right) - 109n_f T_R, \tag{31}$$

with $T_R = 1/2$.

4

The "effective" one-gluon distribution[5] then reads:

$$\overline{\mathbf{f}}(x) = \delta(1-x) + \int_0^1 d\epsilon \int_0^1 dt \left[A_1\alpha_S\left(Q^2\epsilon^2 t\right) + A_2\,\alpha_S^2\left(Q^2\epsilon^2 t\right)\epsilon t + S_1\,\alpha_S\left(Q^2\epsilon^2 t\right)\epsilon + C_1\,\alpha_S\left(Q^2\epsilon^2 t\right)t\right]$$
$$\left[\delta(1-x-\epsilon t) - \delta(1-x)\right]. \tag{32}$$

This integral is no longer symmetric for $\varepsilon \leftrightarrow t$ because of running coupling effects.

A consistent resummation to NLO accuracy (and beyond) is naturally performed in moment space, so that we consider [11]:

$$\overline{\mathbf{f}}_N = \int_0^1 dx\, x^{N-1}\overline{\mathbf{f}}(x)$$
$$= 1 + \Delta\overline{\mathbf{f}}_N. \tag{33}$$

With this definition of the Mellin transform, the total rate is given by the first moment. Note that $\overline{\mathbf{f}}_{N=1} = 1$. The inverse transform to the original distribution in x-space is usually done numerically [12]. The moments of the one-loop distribution $\overline{\mathbf{f}}(x)$ given in eq. (18) read:

$$\overline{\mathbf{f}}_n = 1 - A_1\alpha_S 2\log^2 n - B_1\alpha_S\log n - A_1\pi^2 12\alpha_S + O\left(1n\right). \tag{34}$$

We have defined $n \equiv N/N_0$, where $N_0 \equiv e^{-\gamma_E} = 0.561459\ldots$ with $\gamma_E = 0.577216\ldots$ the Euler constant [6]. The single logarithm, the $\log n$ term, is positive and tends to increase the rate, as is often the case [13]. Its coefficient B_1 is rather big; it is over a factor of 2 larger than in DIS, for example, where C_1 is the same and $S_1 = 0$. Simple exponentiation of the effective one-gluon distribution takes place in N-space, so that

$$\overline{\mathbf{f}}_N = e^{\Delta\overline{\mathbf{f}}_N}. \tag{35}$$

The non-logarithmic integrations of the terms proportional to S_1 and C_1 can be explicitly done [6] and one obtains:

$$\log\overline{\mathbf{f}}_N = \int_0^1 dx\, x^{N-1} - 11 - x\left\{\left[\int_{Q^2(1-x)^2}^{Q^2(1-x)} dq^2 q^2\left[A_1\alpha_S\left(q^2\right) + A_2\alpha_S^2\left(q^2\right)\right] + \right.\right.$$
$$\left.\left. + S_1\alpha_S\left(Q^2(1-x)^2\right) + C_1\alpha_S\left(Q^2(1-x)\right)\right\} + O\left(\alpha_S^n\log^{n-1} N\right), \tag{36}$$

Using the large-N approximation $x^N - 1 \simeq -\theta(1-x-1/n)$ [6][6], the moments read:

$$\log\overline{\mathbf{f}}_n = -A_1 2\beta_0\left[\log s\log\log s - 2\log sn\log\log sn + \log sn^2\log\log sn^2\right] +$$
$$+ \beta_0 A_2 - \beta_1 A_1 2\beta_0^3\left[\log\log s - 2\log\log sn + \log\log sn^2\right] +$$
$$- \beta_1 A_1 4\beta_0^3\left[\log^2\log s - 2\log^2\log sn + \log^2\log sn^2\right] +$$
$$- S_1 2\beta_0\left[\log\log s - \log\log sn^2\right] - C_1\beta_0\left[\log\log s - \log\log sn\right], \tag{37}$$

where s is the square of the hard scale in unit of the QCD scale,

$$s \equiv Q^2\Lambda^2. \tag{38}$$

Note that $\overline{\mathbf{f}}_n = 1$ for $n = 1$. Substituting $\log s$ in eq. (37) by its expression in terms of the two-loop coupling,

$$\log s = 1\beta_0\alpha_S + \beta_1\beta_0^2\log\left(\beta_0\alpha_S\right), \tag{39}$$

---

[5]We call it "effective" because the insertion of the running coupling in the time-like region and of the term proportional to A_2 already includes some multiple-gluon-emission effects.

[6]The error in this approximation amounts to next-to-next-to-leading logarithms and to terms suppressed by powers of $1/N$.

one obtains the exponent (37) as a series of functions [14]:

$$\overline{\mathbf{f}}_n = \exp\left[L\, g_1\left(\beta_0 \alpha_S L\right) + g_2\left(\beta_0 \alpha_S L\right) + \alpha_S\, g_3\left(\beta_0 \alpha_S L\right) + \cdots\right], \tag{40}$$

where the leading and next-to-leading functions are respectively [15]:

$$
\begin{aligned}
g_1(w) &= -A_1 2\beta_0\, \frac{1}{w}\left[(1-2w)\log(1-2w) - 2(1-w)\log(1-w)\right]; \\
g_2(w) &= \beta_0 A_2 - \beta_1 A_1 2\beta_0^3\left[\log(1-2w) - 2\log(1-w)\right] - \beta_1 A_1 4\beta_0^3\left[\log^2(1-2w) - 2\log^2(1-w)\right] + \\
&\quad + S_1 2\beta_0\log(1-2w) + C_1\beta_0\log(1-w).
\end{aligned}
\tag{41}
$$

We have defined $\alpha_S \equiv \alpha_S\left(Q^2\right)$ and $L \equiv \log n$. The two-loop terms coming from the expansion of the resummed distribution read:

$$\log\overline{\mathbf{f}}_n^{\,2loop} = -12A_1\beta_0\,\alpha_S^2\,L^3 - \left(12A_2 + \beta_0 S_1 + 12\beta_0 C_1\right)\alpha_S^2\,L^2. \tag{42}$$

The effective form factor is real — and therefore sensible — only for

$$n < n_{crit} = \exp\left[12\beta_0\alpha_S\left(Q^2\right)\right] \sim Q\Lambda. \tag{43}$$

This restriction is induced by the soft terms — i.e. by those proportional to A_1, S_1 and A_2. The reliability of the resummed result is then limited to

$$n \ll Q\Lambda \qquad \Leftrightarrow \qquad m^2 \gg \Lambda\,Q. \tag{44}$$

The condition is the same as that in the leading order analysis. On the other hand, the hard collinear contribution — the term proportional to C_1 — remains well-defined up to much larger values of n:

$$n \ll n_{crit}^2 \sim Q^2\Lambda^2 \qquad \Leftrightarrow \qquad m^2 \gg \Lambda^2. \tag{45}$$

The collinear factor is therefore well-defined in the kinematic region (11) described by the shape function. It becomes singular only in the resonance or exclusive region $m^2 \sim \Lambda^2$, which is well beyond the reach of the shape function.
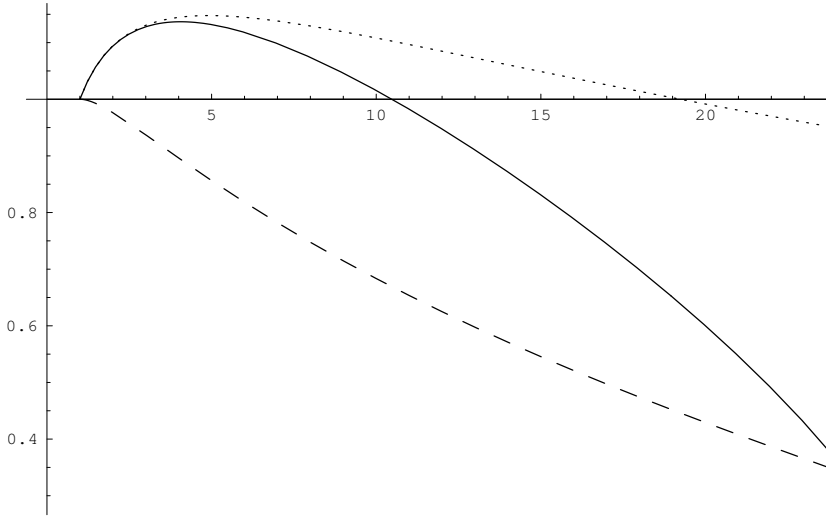
Figure 1: Plot of the QCD form factor $\bar{\mathbf{f}}_n$ as a function of n (first 24 moments) for the values of the parameters discussed in the text. Solid line: NLO distribution; dashed line: LO distribution; dotted line: expansion to order α_S^2 of the exponent in the NLO distribution.

The LO and NLO form factors are plotted in fig. 1 for $Q = m_B \simeq 5.2$ GeV, for which $\alpha_S \simeq 0.21$ and $n_{crit} \simeq 28$. The NLO curve lies above the LO one and it exceeds one in the small-n region because of the single logarithm, as already discussed. The two-loop curve lies above the NLO one because the leading terms in higher orders are all negative (cf. eqs. (34) and (42)).

The resummed distribution is usually written as [16]:

$$\mathbf{f}_N\left(\alpha_S\right) \, = \, K\left(\alpha_S\right)\bar{\mathbf{f}}_N\left(\alpha_S\right) \, + \, D_N\left(\alpha_S\right) , \tag{46}$$

where K is a function with a power series expansion in α_S :

$$K\left(\alpha_S\right) = 1 + k\,\alpha_S \, + k'\alpha_S^2 \, + \cdots \tag{47}$$

and D_N is a remainder function:

$$D_N\left(\alpha_S\right) \, = \, d_N\,\alpha_S + d'_N\,\alpha_S^2 + \cdots, \tag{48}$$

starting at order α_S and vanishing in the large-N limit,

$$D_N \sim 1N \qquad \text{for} \qquad N \to \infty. \tag{49}$$

To NLO accuracy, the contributions of order α_S to the function K (and D_N) are needed. To the same accuracy, in place of (46), one can write $\mathbf{f}_N = \left(1 + \alpha_S\,k + \alpha_S\,d_N\right)\bar{\mathbf{f}}_N$.

An expression analogous to (46) also holds for the distributions in the semileptonic decay (5) with a fixed hadronic energy, i.e. to differential distributions in the hadronic energy. One simply has to make the replacement

$$x \to z \tag{50}$$

7

in eq. (46) and to account for a dependence of K and D_N on Q/m_B. The function $\overline{\mathbf{f}}$ is the same in the semileptonic and in the rare decay:

$$\overline{\mathbf{f}}\,(x) = \overline{\mathbf{f}}\,(z).\tag{51}$$

The general variable for the threshold region of heavy flavour decays is z, even though, for the rare decay (4), it is more convenient to use x. In the semi-inclusive region these two variables concide, because

$$1 - z = 1 - x\,(2-x)^2 = 1 - x + O\left((1-x)^2\right).\tag{52}$$

3 The shape function

Let us now consider the quantity in the effective theory related to $\mathbf{f}\,(z)$, namely the shape function $\varphi\,(k_+)$. The latter has the analogous decomposition:

$$\varphi\,(k_+) = \overline{\varphi}\,(k_+) + \alpha_S\,h\,\delta\,(k_+) + \alpha_S\,p\,(k_+).\tag{53}$$

The function $\overline{\varphi}\,(k_+)$ factorizes long-distance effects and reads:

$$\begin{aligned}\overline{\varphi}\,(k_+) &= \delta\,(k_+) - A_1\alpha_S\,\theta\,(0; k_+; -\mu) - k_+\log -k_+\mu + A_1\alpha_S\,\delta\,(k_+)\int_{-\mu}^{0} dl_+ - l_+\log -l_+\mu +\\ &\quad +S_1\alpha_S\,\theta\,(0; k_+; -\mu) - k_+ - S_1\alpha_S\,\delta\,(k_+)\int_{-\mu}^{0} dl_+ - l_+,\end{aligned}\tag{54}$$

where $\mu \equiv 2\Lambda_S$ and we have defined $\theta\,(a_1; a_2; \cdots a_n) \equiv \theta\,(a_1 - a_2)\,\theta\,(a_2 - a_3)\cdots\theta\,(a_{n-1} - a_n)$. The regularization used [4] imposes a cut-off on the spatial loop momenta and not on the energies,

$$|\overrightarrow{l}\,| < \Lambda_S, \qquad -\infty < l_0 < +\infty,\tag{55}$$

and it is qualitatively similar to lattice regularization[7]. Proceeding in a similar way, one can write:

$$\overline{\varphi}\,(k_+) = \delta\,(k_+) + \int_0^{\mu} dE E \int_0^1 dt\,\left[A_1\alpha_S\,(E^2 t) + A_2\alpha_S^2\,(E^2 t)\,t + S_1\alpha_S\,(E^2 t)\right]\left[\delta\,(k_+ + Et) - \delta\,(k_+)\right].\tag{56}$$

A few comments are in order. The hard scale Q does not appear in $\overline{\varphi}\,(k_+)$, as it should. The term proportional to C_1 is absent because the shape function retains only the leading terms in the soft limit $E \to 0$, which are proportional to $1/E$. With the same definition of the coupling constant in QCD and in the ET, the constant A_2 is the same in the two theories [17, 18][8]. Since $k_+ = -Q\,(1 - z)$, the shape function in the "QCD variable" z reads:

$$\overline{f}\,(z) = \delta\,(1 - z) + \int_0^{1/r} d\epsilon\,\epsilon \int_0^1 dt\,\left[A_1\alpha_S\,(Q^2\epsilon^2 t) + A_2\,\alpha_S^2\,(Q^2\epsilon^2 t)\,t + S_1\alpha_S\,(Q^2\epsilon^2 t)\right]\left[\delta\,(1 - z - \epsilon t) - \delta\,(1 - z)\right],\tag{57}$$

---

[7]By this we mean that the double logarithm at one loop is the same in the two regularizations.
[8]A difference would imply a breakdown of factorization.

where we have defined an adimensional function as

$$\overline{f}(z) \equiv Q \, \overline{\varphi}(k_+).$$ (58)

The quantity r is the ratio of the hard scale to the UV cut-off of the effective theory,

$$r \equiv Q\mu > 1,$$ (59)

because the shape function is defined in a low-energy effective field theory. To avoid substantial finite cut-off effects, one has also to assume

$$\mu \gg \Lambda.$$ (60)

Taking moments and exponentiating the one-loop distribution as in the QCD case, one obtains:
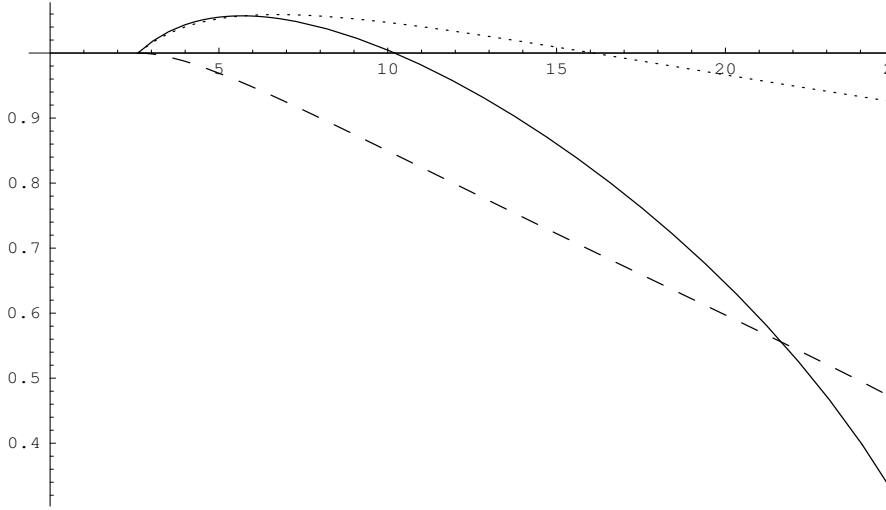
$$\overline{f}_N = e^{\Delta \overline{f}_N}.$$ (61)

Figure 2: Plot of the shape function $\overline{f}_n$ (first 25 moments). Solid line: NLO distribution; dashed line: LO distribution; dotted line: expansion to order α_S^2 of the exponent in the NLO distribution.

Making the same approximations as in the QCD case, the shape function is written:

$$\log \overline{f}_n = -\theta\,(n-r) \int_{1/n}^{1/r} dy\, y \left\{ \int_y^{1/r} d\epsilon\,\epsilon \left[A_1 \alpha_S \left(Q^2 \epsilon y\right) + A_2\,\alpha_S^2 \left(Q^2 \epsilon y\right) \right] + S_1 \alpha_S \left(Q^2 y^2\right) \right\}.$$ (62)

A straightforward integration then gives:

$$
\begin{aligned}
\log \overline{f}_n \;=\;\; & \theta\,(n-r) \left\{ -A_1 2\beta_0 \left[\log s n^2 \log\log s n^2 - 2\log s r\, n \log\log s r\, n + \log s r^2 \log\log s r^2 \right] + \right. \\
& \quad + A_2\beta_0 - A_1\beta_1 2\beta_0^3 \left[\log\log s n^2 - 2\log\log s r\, n + \log\log s r^2 \right] + \\
& \quad \left. - A_1\beta_1 4\beta_0^3 \left[\log^2\log s n^2 - 2\log^2\log s r\, n + \log^2\log s r^2 \right] + S_1 2\beta_0 \left[\log\log s n^2 - \log\log s r^2 \right] \right\}
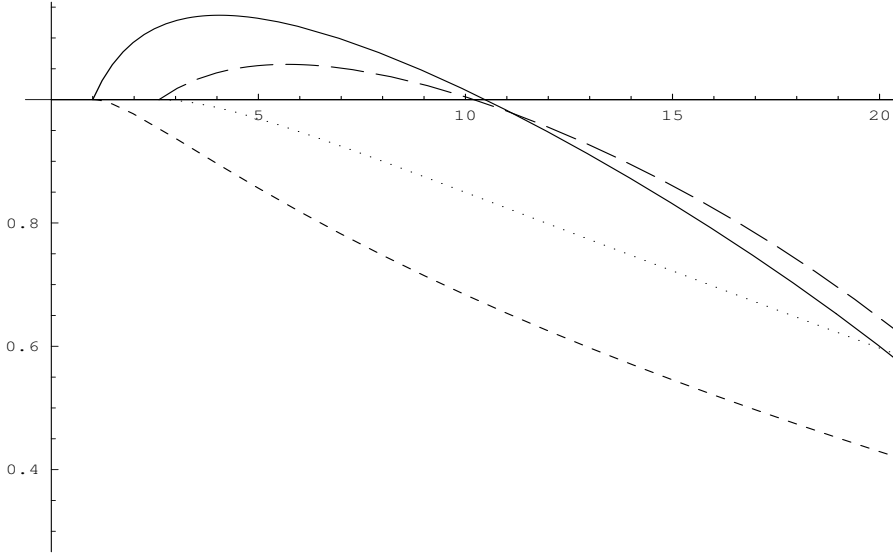\end{aligned}
$$ (63)

9

Figure 3: Comparison of QCD form factor with the shape function. Solid line: NLO QCD distribution; big dashed line: NLO shape function; small dashed line: LO QCD distribution; dotted line: LO shape function.

The main point is that the terms containing n^2 are independent of r: the infrared behaviour is the same as in QCD, as expected on physical grounds. Substituting $\log s$ by its expression in terms of the two-loop coupling, the result reads:

$$\log \overline{f}_n = L \, g_1^{ET} (\beta_0 \alpha_S L; \beta_0 \alpha_S R) + g_2^{ET} (\beta_0 \alpha_S L; \beta_0 \alpha_S R) + \cdots$$

where:

$$
\begin{aligned}
g_1^{ET} (w; \tau) &= -A_1 2\beta_0 w \left[(1 - 2w) \log (1 - 2w) + (1 - 2\tau) \log (1 - 2\tau) - 2 (1 - w - \tau) \log (1 - w - \tau)\right], \\
g_2^{ET} (w; \tau) &= A_2 \beta_0 - A_1 \beta_1 2\beta_0^3 \left[\log(1 - 2w) + \log (1 - 2\tau) - 2 \log (1 - w - \tau))\right] + \\
&\quad - A_1 \beta_1 4\beta_0^3 \left[\log^2(1 - 2w) + \log^2(1 - 2\tau) - 2 \log^2 (1 - w - \tau)\right] + \\
&\quad + S_1 2\beta_0 \left[\log(1 - 2w) - \log(1 - 2\tau)\right],
\end{aligned}
\tag{64}
$$

and

$$R \equiv \log r > 0, \tag{65}$$

and the over-all factor $\theta (L - R)$ has been omitted. Note that $\overline{f}_n$ is continuous at $n = r$, but it has a cusp singularity in this point. The range of n is restricted by eq. (44): the same limitation of the QCD distribution occurs. The QCD form factor $\overline{\mathbf{f}}_n$, except for the C_1 term, is obtained by taking $\tau = 0$ in the above expression, i.e. letting the gluon energy to reach the hard scale. The shape function is plotted in fig. 2 for the same values of the parameters of the QCD distribution and for $\mu = 2 \, \mathrm{GeV}$. In fig. 3 we compare the QCD form factor with the shape function. In NLO, the shape-function curve is below the QCD one for small n because it has no C_1 term. NLO distributions are very close to each other for large n, but this seems accidental; indeed, this phenomenon does not occur for the LO distributions. In general, the shape-function curves look somehow shifted with respect to the corresponding QCD ones.

The moments of the shape function can be decomposed in a form similar to the QCD distribution:

$$f_N (\alpha_S) = H (\alpha_S) \overline{f}_N (\alpha_S) + P_N (\alpha_S), \tag{66}$$

10

where the functions $H(\alpha_S)$ and $P_N(\alpha_S)$ have a power series expansion in α_S :

$$
\begin{aligned}
H(\alpha_S) &= 1 + h\,\alpha_S + h'\alpha_S^2 + \cdots \\
P_N(\alpha_S) &= p_N\,\alpha_S + p'_N\,\alpha_S + \cdots .
\end{aligned}
\tag{67}
$$

To NLO accuracy, an expression alternative to (66) including higher-twist effects is $f_N = (1 + \alpha_S\,h + \alpha_S\,p_N)\,\overline{f}_N$.

4 The coefficient function

We introduce the coefficient function C_N relating the shape function to the QCD form factor, as

$$
\mathbf{f}_N = C_N\,f_N.
\tag{68}
$$

Inserting the expressions previously obtained and neglecting the remainder functions D_N and P_N, the coefficient function reads:

$$
C_N(\alpha_S) = G(\alpha_S)\,\Sigma_N(\alpha_S),
\tag{69}
$$

where

$$
G(\alpha_S) = K(\alpha_S)\,H(\alpha_S) = 1 + g\,\alpha_S + \cdots
\tag{70}
$$

and

$$
\Sigma_N(\alpha_S) = \overline{\mathbf{f}}_N(\alpha_S)\,\overline{f}_N(\alpha_S)
\tag{71}
$$

with $g = k - h$. To NLO accuracy, the replacement $G(\alpha_S) \to 1 + \alpha_S\,g + \alpha_S\,(d_N - p_N)$ is allowed, including also the remainder terms. The QCD distribution and the shape function are related by a convolution in momentum space:

$$
\mathbf{f}(z) = \int_0^1\int_0^1 dz'dz''\delta(z - z'z'')\,C(z')\,f(z'').
\tag{72}
$$

The function Σ_n reads:

$$
\log\Sigma_n = \theta(r - n)\log\overline{\mathbf{f}}_n + \theta(n - r)\left[\log\overline{\mathbf{f}}_n - \log\overline{f}_n\right].
\tag{73}
$$

The explicit expression for $n > r$ is:

$$
\log\Sigma_n = L\,g_1^{CF}(\beta_0\alpha_S L;\ \beta_0\alpha_S R) + g_2^{CF}(\beta_0\alpha_S L;\ \beta_0\alpha_S R) + \cdots,
\tag{74}
$$

where

$$
\begin{aligned}
g_1^{CF}(w;\tau) &= -A_1 2\beta_0 w\left[2(1 - w - \tau)\log(1 - w - \tau) - 2(1 - w)\log(1 - w) - (1 - 2\tau)\log(1 - 2\tau)\right]; \\
g_2^{CF}(w;\tau) &= A_2\beta_0 - A_1\beta_1 2\beta_0^3\left[2\log(1 - w - \tau) - 2\log(1 - w) - \log(1 - 2\tau)\right] + \\
&\quad -A_1\beta_1 4\beta_0^3\left[2\log^2(1 - w - \tau) - 2\log^2(1 - w) - \log^2(1 - 2\tau)\right] + \\
&\quad +S_1 2\beta_0\log(1 - 2\tau) + C_1\beta_0\log(1 - w).
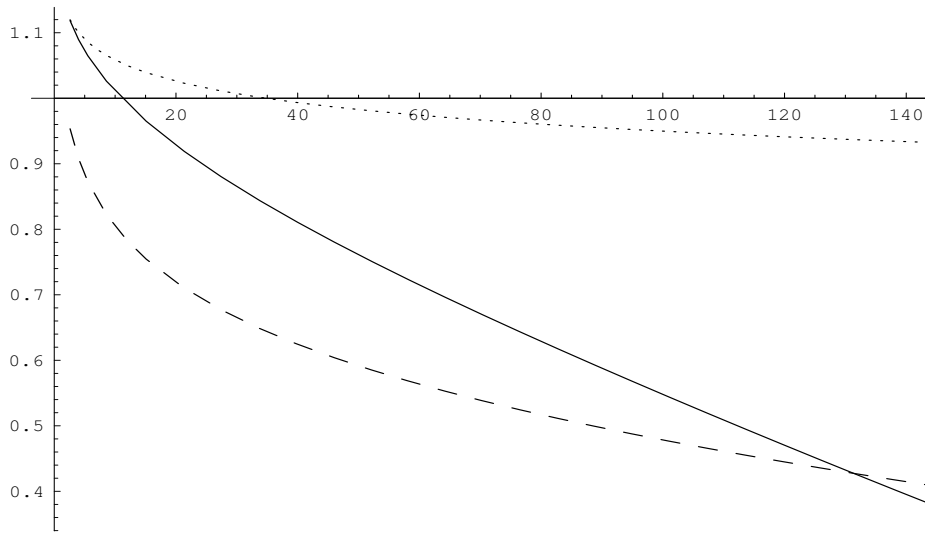\end{aligned}
\tag{75}
$$

Figure 4: Plot of the coefficient function Σ_n for the choice of the parameters discussed previously (first 140 moments). Solid line: NLO distribution; dashed line: LO distribution; dotted line: expansion to order α_S^2 of the exponent in the NLO distribution.

Equation (75) is our main result. Let us comment on it. The terms most affected by long-distance effects are those containing the combination $1 - 2w$ and they are the same in QCD and in the ET. As a consequence, they cancel in the difference, proving that the coefficient function is short-distance-dominated to NLO accuracy; we believe that this cancellation occurs to any order in PT. The coefficient function is meaningful up to

$$n \ll n'_{crit} = \mu Q \exp\left[1\beta_0\, \alpha_S\left(Q^2\right)\right] \sim \mu Q \Lambda^2. \tag{76}$$

Note that n'_{crit} lies between the critical values for the soft terms and the hard collinear one:

$$n_{crit} \ll n'_{crit} \ll n_{crit}^2. \tag{77}$$

The coefficient function contains also the jet factor, entirely coming from the QCD form factor:

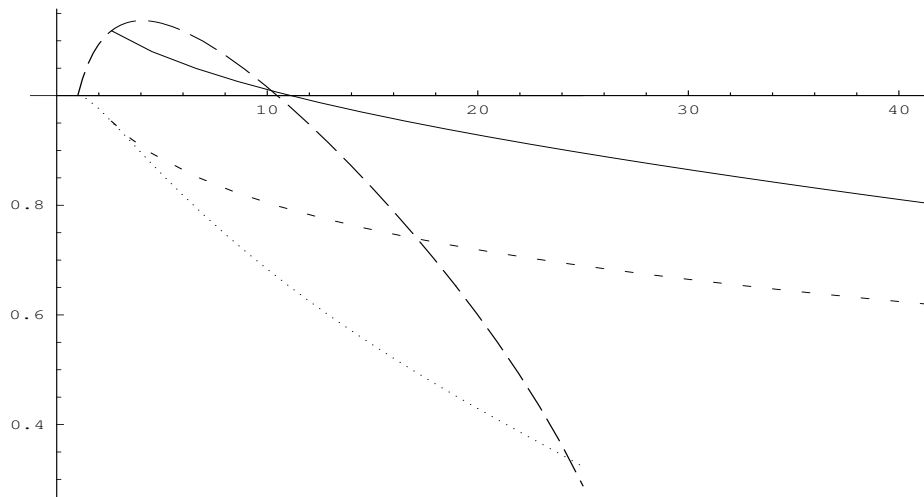$$J_n = \exp\left[C_1\beta_0 \log(1 - w)\right]. \tag{78}$$

12

Figure 5: Comparison of the coefficient function with the QCD form factor. Solid line: NLO coefficient function; big dashed line: NLO QCD distribution; small dashed line: LO coefficient function; dotted line: LO QCD distribution.

The coefficient function is plotted in fig. 4 for the values of the parameters specified previously. It becomes singular at $n'_{crit} \cong 297$, i.e. an order of magnitude above the QCD form factor or the shape function. For $n \lesssim 50$, the NLO curve has a shape similar to the LO one and it is shifted up with respect to the latter by ~ 0.2. In fig. 5 we compare the coefficient function with the QCD form factor. Note that the large-N approximation produces a cusp singularity in the NLO coefficient function at $n = r$.

The computation of the shape function from first principles — namely lattice QCD — requires a large amount of theoretical work, consisting of the following steps:

1. analytic continuation from Euclidean to Minkowski space of the relevant correlation function, a 4-point function;

2. lattice regularization of the effective theory in which the shape function is defined, which involves the HQET (Wilson lines *off* the light cone) and the LEET (Wilson lines *on* the light-cone);

3. computation of the shape function in lattice perturbation theory to full order α_S;

4. matching of the lattice shape function with the QCD distribution to full order α_S;

5. Numerical computation with a Monte Carlo program of the correlation function on the lattice.

The first step was taken in ref. [19], showing the possibility of a lattice computation of the shape function. Step 2 has only partially been completed: the lattice HQET has been formulated in ref. [20] while the lattice LEET — as far as we know — has not been constructed yet. The main difference is that, in the latter case, not only soft singularities but also light-cone singularities appear in the euclidean correlation functions; we do not attempt at the construction of the lattice LEET here. No theoretical work exists — as far as we know — on points 3, 4 and 5. In general, a lot of work is yet to be done: the purpose of this note was simply showing how to resum to all orders the threshold logarithms appearing in the coefficient function.

Our result (75) applies to the coefficient function of the shape function defined in lattice regularization, after the identification is done:

$$1a = c\,\mu, \tag{79}$$

13

where c is a constant or order 1 and a is the lattice spacing. c is determined, for example, imposing the equality of the coefficients of the single logarithms in the lattice shape function and in eq. (53) (steps 3 and 4). In our work, we have *assumed* the consistency of the lattice LEET and the *knowledge* of the one-loop lattice amplitude.

In the absence of a (non-perturbative) computation of the shape function, we can compare our coefficient function evaluated with a cut-off of a few times the hadronic scale (in practice $1 \div 2$ GeV) directly with the experimental data. The mismatch is the non-perturbative component up to a scale μ, namely the shape function. The factorization scale μ acts effectively in the coefficient function as a prescription for the Landau pole. In this respect, our coefficient function can be considered as a complete QCD form factor, with a prescription to remove the Landau pole outside region (11). As we have seen, the singularity is not completely removed, but it is shifted to much larger values of N. We stress that our splitting of the QCD form factor into a coefficient function and a shape function represents a consistent separation of perturbative from non-perturbative effects; it somehow differs from the usual strategy of finding a good prescription for the running coupling in the non-perturbative region.

5   Conclusions

We have presented a NLO evaluation of the resummed coefficient function for the shape function. Our result, together with a one-loop lattice computation that is still missing, allows relating the shape function computed with lattice QCD to distributions in heavy-flavour decays in the semi-inclusive region (11). The NLO analysis corroborates the results of the leading order one, but it does not reveal any new qualitative feature. The coefficient function is short-distance-dominated in the relevant region (11), and corrections to factorization are expected to be of the order Λ/μ, i.e. to involve one inverse power of the factorization scale. The NLO coefficient function contains also a jet factor that takes into account the emission of hard collinear gluons. The latter process is indeed not described by the effective theory, which takes into account only soft emission up to the scale μ. On the quantitative side, NLO effects increase the coefficient function by $\sim 20\%$ for $\mu = 2$ GeV and $n \lesssim 50$ in the case of B decays.

In general, the process (1) contains three different scales:[9]

$$
\begin{array}{rlcl}
i) & Q^2 & \gg & \Lambda^2, \\
ii) & Q\,k_+ & \sim & Q\,\Lambda \gg \Lambda^2, \\
iii) & k_+{}^2 & \sim & \Lambda^2.
\end{array}
\tag{80}
$$

The emission of gluons with transverse momenta ranging between $i)$ and $ii)$ is reliably computed in perturbation theory, while fluctuations in region $iii)$ ask for a non-perturbative treatment. With factorization by means of the shape function, another scale is introduced in the problem, intermediate between $ii)$ and $iii)$:

$$
iv) \quad \mu\,k_+ \sim \mu\,\Lambda \gg \Lambda^2.
\tag{81}
$$

The fluctuations between scales $iii)$ and $iv)$ are factorized in the shape function. The general idea behind the shape-function approach is that soft contributions are more "non-perturbative" than collinear ones in double-logarithmic problems in region (11), because they involve smaller transverse momenta. These soft non-perturbative effects can be represented as hadronic matrix elements of non-local operators involving Wilson lines. For a given process, one identifies a dominant kinematical configuration and replaces the hard partons with Wilson lines with the same momenta.

To summarize, we have presented a NLO evaluation of the resummed coefficient function of the shape function, which confirms the consistency of the effective theory approach and allows a more accurate theoretical analysis.

---

[9]I wish to thank G. Korchemsky for a discussion on this point.

References

[1] U. Aglietti, preprint CERN-TH/2001-035, hep-ph/0102138.

[2] G. Altarelli, N. Cabibbo, G. Corbó, L. Maiani and G. Martinelli, Nucl. Phys. B 208, 365 (1982).

[3] I. Bigi, M. Shifman, N. Uraltsev and A. Vainshtein, Phys. Rev. Lett. 71, 496 (1993); Int. J. Mod. Phys. A 9, 2467 (1994); A. Manohar and M. Wise, Phys. Rev. D 49, 1310 (1994); M. Neubert, Phys. Rev. D 49, 3392 and 4623 (1994); T. Mannel and M. Neubert, Phys. Rev. D 50, 2037 (1994).

[4] U. Aglietti and G. Ricciardi, Phys. Lett. B 466, 313 (1999); Nucl. Phys. B 587, 363 (2000).

[5] C. Bauer, S. Fleming and M. Luke, Phys. Rev. D 63, 014006 (2001).

[6] S. Catani and L. Trentadue, Nucl. Phys. B 327, 323 (1989).

[7] U. Aglietti, invited talk at the *QCD 00 Euroconference,* Montpellier, 6-12 July 2000, to appear in the proceedings.

[8] A. Ali and C. Greub, Z. Phys. C 49, 431 (1991) and Phys. Lett. B 259, 182 (1991); A. Kapustin and Z. Ligeti, Phys. Lett. B 355, 318 (1995); A. Falk, M. Luke and M. Savage, Phys. Rev. D 49, 3367 (1994); N. Pott, Phys. Rev. D 54, 938 (1996); C. Greub, T. Hurth and D. Wyler, Phys. Lett. B 380, 385 (1996) and Phys. Rev. D 54, 3350 (1996).

[9] D. Amati, A. Bassetto, M. Ciafaloni, G. Marchesini and G. Veneziano, Nucl. Phys. B 173, 429 (1980).

[10] J. Kodaira and L. Trentadue, preprint SLAC-PUB-2934 (1982); Phys. Lett. B 112, 66 (1982); S. Catani, E. D'Emilio and L. Trentadue, Phys. Lett. B 211, 335 (1988).

[11] See for example, S. Catani, Proceedings of the *QCD 96 Euroconference*, Montpellier, France, July 1996.

[12] S. Catani, M. Mangano, L. Trentadue and P. Nason, Nucl. Phys. B 478, 273 (1996).

[13] J. Kodaira and L. Trentadue, Phys. Lett. B 123, 335 (1983) and B 151, 171 (1985).

[14] S. Catani and L. Trentadue, Nucl. Phys. B 353, 183 (1991).

[15] R. Akhouri and I. Rothstein, Phys. Rev. D 54, 2349 (1996); G. Korchemsky and G. Sterman, Phys. Lett. B 340, 96 (1994).

[16] S. Catani, L. Trentadue, G. Turnock and B. Webber, Nucl. Phys. B 407, 3 (1993).

[17] S. Catani, G. Marchesini and B. Webber, Nucl. Phys. B 349, 635 (1991).

[18] G. Korchemsky and G. Marchesini, Nucl. Phys. B 406, 225 (1993).

[19] U. Aglietti, M. Ciuchini, G. Corbó, E. Franco, G. Martinelli and L. Silvestrini, Phys. Lett. B 432, 411 (1998).

[20] P. Boucaud, C. Lime and O. Pène, Phys. Rev. D 40, 1525 (1989); E. Eichten and B. Hill, Phys. Lett. B 240, 193 (1990); U. Aglietti, Nucl. Phys. B 421, 191 (1994).